The Fate of Alkane Radical Cations in Liquid and Solid Hydrocarbons. Time-Resolved Fluorescence Detected Magnetic Resonance†

D. W. Werst, M. G. Bakker, and A. D. Trifunac*

Contribution from the Chemistry Division, Argonne National Laboratory, Argonne, Illinois 60439. *Received May 18, 1989*

Abstract: Time-resolved fluorescence detected magnetic resonance (FDMR) is used to observe alkane radical cations generated by electron radiolysis in liquid and solid alkane solutions. The ease of observation of the alkane radical cations (on the time scale of tens to hundreds of nanoseconds) depends strongly on the alkane under study as well as the conditions of temperature and concentration. Ion–molecule reactions such as proton transfer or H-atom transfer are responsible for the very transient nature of the alkane radical cations and possibly account for much of the diversity of hydrocarbon radiation chemistry.

1. Introduction

Radical ions have been studied in a variety of contexts by organic and physical chemists. The reactivity of electron-loss species and electron-gain species are important in electron-transfer and redox reactions generally. The importance of electron-loss species, radical cations, is increasingly appreciated as we are becoming aware of their ubiquitous presence in chemistry induced by energetic radiation, both ionizing and photoionizing. With the advent of techniques allowing real time studies of very transient species in the condensed phase, it has become apparent that ions and their reactions play a decisive role in the chemistry induced by energetic radiation, with consequences for our perceptions of widely diverse areas of chemistry.

Within the limits of state-of-the-art time domain studies, radical cations and their geminate electron partners are thought to be the primary chemical entities produced by energetic radiation. Essentially all of the subsequent chemistry follows from the spatial distribution of the cation–electron pairs and further transformations of the radical cations. The problem is that very few real time studies of radical cation chemistry in the condensed phase have been carried out. Only a handful of nanosecond optical and conductivity studies and even fewer picosecond optical studies exist. All EPR studies have been restricted to the study of static systems where stabilization of radical cations is achieved. While these EPR studies have been essential in identifying the details of the structure of radical cations, insights into radical cation chemistry have been limited by complications of matrix chemistry. Nevertheless, EPR experiments employing specialized matrix methods have enumerated many of the conceivable reaction pathways of radical cations. What is left is to assess the relative importance of such condensed-phase reactions of radical cations in more realistic reaction systems.

Alkane radical cations ($RH^{\bullet+}$) are σ-radical cations, a fundamentally important class of organic intermediates. They occur in hydrocarbon radiolysis and their chemistry is prototypical of processes occurring in radiation modification of polymers and has considerable relevance to the understanding of the biological effects of ionizing radiation. In the last decade much has been learned about the geometry and electronic structure of $RH^{\bullet+}$ species formed by positive charge transfer and stabilized in irradiated frozen matrices such as $CFCl_3$, and other halocarbons using static EPR spectroscopy.[1] Unfortunately, conventional CW EPR methods are unable to detect $RH^{\bullet+}$ species in neat alkanes, even at 4 K.[2] It is assumed that very rapid conversion of alkane radical cations into alkyl radicals occurs. Alkyl radicals are ubiquitous in irradiated alkanes and are easily detected by EPR.

Several studies have been described in which transient absorptions observed in the visible region in pulse radiolysis of alkanes are assigned to the parent radical cations.[3-9] In these experiments, the signals ascribed to the parent radical cations undergo more rapid decay than absorbances in the region 1.5–3.5 μm due to solvated electrons. This suggests a decay channel for alkane radical cations in addition to recombination. Interpretation of these results, however, is inherently difficult owing to the lack of structural features in the absorption spectra and possible interference from other absorbing species.

Recent studies using the technique of microwave modulation of fluorescence resulting from the recombination of charge pairs provided the first direct EPR observation of alkane radical cations in irradiated hydrocarbons. Fluorescence detected magnetic resonance (FDMR) spectroscopy provides an EPR signature of radical ion species which geminately recombine to give fluorescence. Time-resolved FDMR-detected EPR spectra of the *cis*-decalin and norbornane radical cations were observed in dilute liquid alkane solutions.[10] Detection of solvent radical cations in *neat* alkanes by FDMR becomes possible in low-temperature solids, as was demonstrated in frozen decalins.[11-13] These results open the way for the systematic study of the structure and reactivity of alkane radical cations in hydrocarbon media and the elucidation of their role in hydrocarbon radiation chemistry.

The success of FDMR in studies of short-lived radical cations is due to its superior sensitivity and time domain capability relative to conventional EPR methods and to its high degree of spectral resolution (hyperfine structure) compared to condensed-phase optical experiments. FDMR detection of a radical cation requires that it be a constituent of a spin-correlated radical ion pair which yields an excited emitting state upon recombination. Ionizing radiation creates (singlet-phased) radical ion pairs in alkane solvents composed of a solvent radical cation and an electron. Pairs which recombine geminately ($\simeq$95%) will be spin-correlated. In liquid hydrocarbons geminate electron recombination occurs in 1 to 10 ps. Addition of an aromatic scintillator (A) serves the

† Work performed under the auspices of the Office of Basic Energy Sciences, Division of Chemical Science, US-DOE under Contract No. W-31-109-ENG-38.

(1) For a review see: Shiotani, M. *Magn. Res. Rev.* **1987**, *12*, 333.
(2) Iwasaki, M.; Toriyama, K.; Fukaya, M.; Muto, H.; Nunome, K. *J. Phys. Chem.* **1985**, *89*, 5278.
(3) Klassen, N. V.; Teather, G. G. *J. Phys. Chem.* **1979**, *83*, 326.
(4) Teather, G. G.; Klassen, N. V. *J. Phys. Chem.* **1981**, *85*, 3044.
(5) Klassen, N. V.; Teather, G. G. *J. Phys. Chem.* **1985**, *89*, 2048.
(6) Mehnert, R.; Brede, O.; Naumann, W. *Ber. Bunsenges. Phys. Chem.* **1984**, *88*, 71.
(7) Mehnert, R.; Brede, O.; Cserep, G. *Radiat. Phys. Chem.* **1985**, *26*, 353.
(8) LeMotais, B. C.; Jonah, C. D. *Radiat. Phys. Chem.*, in press.
(9) Tagawa, S. *Proceedings of the International Symposium on the Radiation Chemistry of Polymers*, March 1989, Sanjyou-Kaikan, University of Tokyo, Japan. Tagawa, S.; Yoshida, Y.; Hayashi, N.; Washio, M.; Tabata, Y. *Proceedings of the International Symposium on Fast Excitation Processes*, March, 1988, Sanjyou-Kaikan, University of Tokyo, Japan.
(10) Werst, D. W.; Trifunac, A. D. *J. Phys. Chem.* **1988**, *92*, 1093.
(11) Werst, D. W.; Percy, L. T.; Trifunac, A. D. *Chem. Phys. Lett.* **1988**, *153*, 45.
(12) Trifunac, A. D.; Werst, D. W.; Percy, L. T. *Radiat. Phys. Chem.*, in press.
(13) Melekhov, V. I.; Anisimov, O. A.; Veselov, A. V.; Molin, Yu. N. *Chem. Phys. Lett.* **1986**, *127*, 97.

0002-7863/90/1512-40$02.50/0

dual purpose of scavenging a few percent of the electrons, converting them to less mobile scintillator anions, and increasing the quantum yield of recombination fluorescence. The pertinent reactions are the following

$$RH \xrightarrow[\text{beam}]{e^-} RH^{\bullet+} + e^- \quad (1)$$

$$A + e^- \rightarrow A^{\bullet-} \quad (2)$$

$$A + RH^{\bullet+} \rightarrow A^{\bullet+} + RH \quad (3)$$

$$RH^{\bullet+} + e^- \rightarrow RH^* \quad (4)$$

$$A^{\bullet+} + e^- \rightarrow A^* \quad (5)$$

$$A^{\bullet+} + A^{\bullet-} \rightarrow A^* + A \quad (6)$$

$$RH^{\bullet+} + A^{\bullet-} \rightarrow RH + A^* \quad (7)$$

$$^1A^* \rightarrow A + h\nu \quad (8)$$

where RH* and A* denote electronically excited states whose spin multiplicities (singlet or triplet) depend on the relative spin orientation of the partners at the moment of recombination. Application of a microwave pulse at resonant magnetic field reduces the number of singlet-recombining pairs by inducing EPR transitions between the doublet levels of the separated ions, accelerating the mixing of singlet and triplet pair states. Therefore, the absorption of resonant microwaves causes a decrease in the fluorescence intensity because initially created singlet pairs are converted to triplet pairs which give the nonfluorescent triplet state ($^3A^*$) upon recombination. The FDMR spectrum which is the magnetic field dependence of the fluorescence intensity contains a superposition of the EPR spectra of radical ions which were present during the microwave pulse and recombined geminately to give A*.

The minimum lifetime of detectable ions is determined by the time needed ($\simeq$10 to 20 ns) to perturb the ion-pair spin-state populations with a microwave pulse. Therefore, the reactions primarily responsible for the FDMR signal in liquids are (6) and (7). The slowing of diffusion can markedly alter the relative contributions of reactions 5 through 7 to the FDMR signal in frozen solids. With anthracene-d_{10} used as scintillator, the only radical ion species which will give rise to resolvable EPR features in the FDMR spectrum are the alkane radical cations ($RH^{\bullet+}$). The EPR spectra of alkane radical cations range in total width from 150 to 300 G and are centered at approximately $g = 2$. Signals from all other radical ion species in reactions 5–7 ($A^{\bullet+}$, $A^{\bullet-}$, e^-) overlap in a single narrow line also centered at approximately $g = 2$.

Previous work on FDMR has examined the role of S–T mixing[14a] in the radical ion pairs and microwave power dependence.[14b] The spin relaxation process in the radical ion pairs are not significant factors in the loss of spin coherence in the submicrosecond time regime. The main route of disappearance of radical cations is by reaction with their geminate partners. Only the chemical reactions and/or transformations of radical cations which can compete with the geminate recombination can affect the FDMR spectra of radical cations. Thus, FDMR comparisons of radical cations of closely related systems like alkanes are feasible.

Here we propose to assess the relative importance of radical cation reactions in the condensed phase. After examining in some detail the observability (longevity) of radical cations in the condensed phase, we conclude that *ion–molecule reactions* play a significant and intricate role in the fate of radical cations and provide a convenient framework within which we can begin to understand the apparent diversity of hydrocarbopn radiation chemistry.

In this paper we describe the observations of alkane radical cations in liquid and solid hydrocarbon solutions. Following a necessary discussion of the spectroscopic identification of radical cations observed by FDMR in section 3.1, we show how the conditions (temperature and dilution), which allow observations of alkane radical cations on the time scale of tens to hundreds of nanoseconds, reveal the fate of radical cations and illustrate the diversity of their chemistry. While the present work is mainly concerned with understanding the chemistry induced by the ionizing radiation, the reactivity of alkane radical cations and the ion–molecule reactions that they undergo are relevant to a broad area of condensed-phase chemistry.

2. Experimental Section

The 3-MeV electron Van de Graaff ionizing source and pulsed X-band EPR spectrometer used to obtain time-resolved FDMR spectra have been described elsewhere.[14,15] Detailed descriptions of new modifications to our apparatus to allow FDMR experiments to be carried out in low-temperature solids were published recently.[11,16] Coincident with the arrival of the electron beam pulse ($t = 0$), a 100-ns microwave pulse is applied, i.e., from $t = 0$ to $t = 100$ ns. The fluorescence signal is integrated by a boxcar detector gated open between $t = 100$ ns and $t = 200$ ns. The FDMR spectrum is obtained by sweeping the magnetic field at fixed microwave frequency. Signal-to-noise improvement is achieved by averaging many pulses per field setting and averaging over many sweeps. The actual signal is the difference between the fluorescence intensity measured with and without the microwave pulse. In this way noise due to small fluctuations in the electron beam current is reduced.

In the liquid-phase experiments the sample solution (volume = 150 cm^3) was continuously flowed and recirculated through a cylindrical vacuum-jacketed Suprasil EPR cell mounted in the resonant cavity of the spectrometer. Oxygen was eliminated from the sample by continuous bubbling with argon. A 12-ns electron beam pulse of approximately 10^{-10} C (corresponding to approximately 10^{13} ionization events) was used at a repetition rate of 720 pulses/s. If not explicitly stated, the liquid-phase FDMR spectra were obtained at 190 K. The scintillator (anthracene-d_{10}) concentration used was 10^{-4} M.

In the solid-phase experiments the sample consisted of approximately 0.5 cm^3 of an alkane solution in a 4-mm o.d. Suprasil EPR cell. The sample height could be varied via a remotely controlled stepper motor-driven mount.[16] The sample was kept at a constant height during one sweep and then translated 3–4 mm to expose an unirradiated volume. The magnetic field was swept in opposite directions on alternate sweeps which assured that the averaged spectrum was free of baseline slope and artifacts in the relative peak intensities due to degradation of the sample. Samples were degassed by the freeze–pump–thaw method prior to irradiation. A 5-ns electron beam pulse of approximately 10^{-11} C was used at a repetition rate of 60 pulses/s. Except where stated to the contrary, solid-phase FDMR spectra were obtained at 35 K. The scintillator (anthracene-d_{10}) concentration used was 10^{-3} M.

Static EPR measurements were made on a Varian E109 spectrometer with 100-kHz field modulation. Data collection was assisted by the use of an Apple IIe computer. An Air Products LTR-3 liquid transfer Heli-Tran refrigerator was used for temperature control (in the static EPR experiments as well as the solid-phase FDMR experiments). Alkane radical cations were generated in solutions of 1 mol % alkane in $CFCl_3$ (degassed by the freeze–pump–thaw method) by ^{60}Co γ-irradiation.

The alkanes used in this study were purchased from one of the following sources: Aldrich, Phillips, Burdick & Jackson, or Wiley Organics. Purification of these compounds was performed by passing through activated silica gel. In some cases where the unpurified solvent tested free of unsaturated impurities using a UV cutoff (absorbance of 1 in a 1-cm cell) of 200 nm or shorter as the criterion, the solvent was used as received. This practice was mainly limited to the bulk "high-purity" solvents from Burdick & Jackson (e.g., *n*-pentane, *n*-hexane, cyclopentane, cyclohexane). Anthracene-d_{10} and $CFCl_3$ were used as received from Aldrich.

3. Results and Discussion

We have observed the FDMR spectra of a wide variety of alkane radical cations over a range of experimental conditions. In this section, we present a comprehensive summary of our observations of $RH^{\bullet+}$ species in electron-irradiated hydrocarbons. The initial emphasis is on spectral assignments, followed by a description of how the FDMR signal intensity varies with temperature, concentration, and different alkanes. See Table I for

(14) (a) Smith, J. P.; Trifunac, A. D. *J. Phys. Chem.* **1981**, *85*, 1645. (b) Smith, J. P.; Trifunac, A. D. *Chem. Phys. Lett.* **1981**, *83*, 195.

(15) Trifunac, A. D.; Smith, J. P. *The Study of Fast Processes and Transient Species by Electron Pulse Radiolysis*; Baxendale, J. H., Busi, F., Eds.; Reidel: Boston, 1981; p 179.

(16) Werst, D. W.; Percy, L. T.; Trifunac, A. D. *J. Magn. Reson.*, in press.

Table I. ^{1}H Hyperfine Coupling Constants of Alkane Radical Cations[a]

parent compound	T (K)	solvent	a (G)[b]	ref
		Liquid Phase		
cis-decalin	190	*n*-pentane	51 ± 1 (4)	10
norbornane	190	*n*-pentane	65 ± 1 (4)	10
2,2,3,3-tetramethylbutane	190	*n*-pentane	12.2 ± 0.5 (18)	this work
bicyclopentyl	190	*n*-pentane	31.2 ± 0.5 (8)	this work
			15.6 ± 0.5 (2)	this work
cis-bicyclo[4.3.0]nonane	190	*n*-pentane	61 ± 1 (2)	this work
			23 ± 1 (2)	
			8 ± 1 (2)	
trans-bicyclo[4.3.0]nonane	190	*n*-pentane	67 ± 1 (2)	this work
			26 ± 1 (2)	
methylcyclohexane	190	*n*-hexane	48 ± 1 (4)	this work
			13 ± 1 (3)	
cis-1,4-dimethylcyclohexane	190	*n*-pentane	52 ± 1 (4)	this work
trans-1,4-dimethylcyclohexane	190	*n*-pentane	52 ± 1 (4)	this work
parent compound	T (K)	matrix[c]	a (G)[b]	ref
		Solid Phase		
n-pentane	35	*n*-pentane	60 ± 1 (2)	this work
	77	$CFCl_2CF_2Cl$	57 (2)	17
n-hexane	35	*n*-hexane	41 ± 1 (2)	this work
	77	$CFCl_2CF_2Cl$	41 (2)	18
	77	$CFCl_3$	44 (2)	18
			4.1 (8)	
n-heptane	35	*n*-heptane	31 ± 1 (2)	this work
	77	$CFCl_2CF_2Cl$	30 (2)	17
n-octane	35	*n*-octane	22 ± 2 (2)[d]	this work
	77	$CFCl_2CF_2Cl$	22 (2)	17
n-nonane	35	*n*-nonane	17 ± 2 (2)[d]	this work
	77	$CFCl_2CF_2Cl$	17 (2)	17
2-methylhexane	35	2-methylhexane	44 ± 2 (2)	this work
	80	$CFCl_3$	41 ± 1 (2)	this work
3-methylpentane	77	$CFCl_2CF_2Cl$	52.9 (1)	19
			49.9 (1)	
			39.3 (1)	
	77	CF_2BrCF_2Br	52.5 (1)	20
			36.0 (1)	
3-methylhexane	80	$CFCl_3$	43 ± 1 (2)	this work
	77	$CFCl_2CF_2Cl$	57.1 (1)	19
			39.1 (1)	
cis-decalin	45	*cis*-decalin	51 ± 1 (4)	11
trans-decalin	45	*trans*-decalin	52 ± 1 (4)	11
norbornane	100	$CFCl_2CF_2Cl$	65.1 (4)	21
			3.5 (2)	
cis-bicyclo[4.3.0]nonane	135	$CFCl_3$	61 ± 1 (2)	this work
			24 ± 1 (2)	
			7 ± 1 (1)	
2,2,3,3-tetramethylbutane	55	$CFCl_3$	27.5 ± 1 (6)	this work
	140	$CFCl_3$	12.2 ± 0.5 (18)	this work
	77	$CFCl_2CF_2Cl$	29 (6)	18
	77	$CFCl_3$	28.8 (6)	18
			3.8 (12)	
bicyclopentyl	150	$CFCl_3$	32 ± 1 (8)	this work
			16 ± 1 (2)	
			48 ± 1 (4)[e]	
			16 ± 1 (4)[e]	
tricyclo[5.2.1.0^{2,6}]decane	145	$CFCl_3$	15.5 ± 1 (6)	this work
			7 ± 1 (1)	
methylcyclohexane	140	CF_3-c-C_6F_{11}	48.8 (2)	22
			42.7 (2)	
			20.1 (2)	
cis-1,4-dimethylcyclohexane	35	*cis*-1,4-dimethylcyclohexane	53 ± 2 (4)	this work
trans-1,4-dimethylcyclohexane	77	CF_3-c-C_6F_{11}	56.2 (4)	22
cis-1,2-dimethylcyclohexane	35	*cis*-1,2-dimethylcyclohexane	62 ± 5 (2)	this work
			30 ± 5 (2)	
	75	$CFCl_3$	59 ± 1 (2)	this work
			31 ± 1 (2)	
trans-1,2-dimethylcyclohexane	35	*trans*-1,2-dimethylcyclohexane	62 ± 5 (2)	this work
			30 ± 5 (2)	
	77	CF_3-c-C_6F_{11}	59.3 (2)	22
			33.4 (2)	

[a] The hyperfine parameters determined in the present study were obtained from (isotropic) simulations of the data. Parameters were chosen which gave the best fit of the experimental spectrum. They are not in every case purported to be rigorous assignments of the hyperfine couplings. [b] Numbers in parentheses are the number of equivalent protons. [c] Results in hydrocarbon solvents are FDMR experiments; those in halogenated matrices are static EPR experiments. [d] Estimated from simulations of the spectrum using a Gaussian line width equal to that used to simulate the FDMR spectrum observed in *n*-hexane (12 G). [e] Alternative assignment.

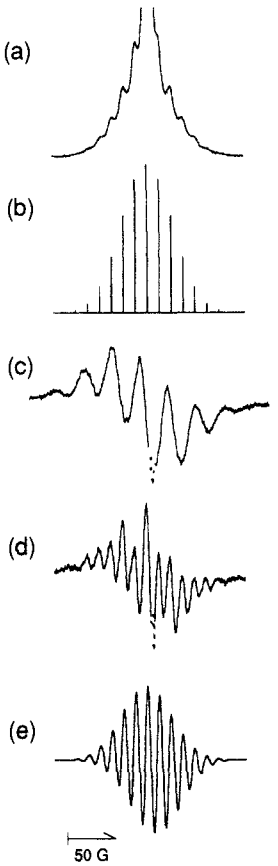

Figure 1. Spectra of the 2,2,3,3-tetramethylbutane radical cation: (a) FDMR spectrum observed at 190 K in *n*-pentane containing 10^{-2} M 2,2,3,3-tetramethylbutane; (b) simulated stick spectrum of (a) using the parameters in Table I; (c) static EPR spectrum observed at 55 K in $CFCl_3$; (d) static EPR spectrum observed at 140 K in $CFCl_3$; (e) simulated spectrum of (d) using the parameters in Table I. The broken line in (c) and (d) is due to a color center in the sample cell.

a compilation of the hyperfine coupling constants (a) of alkane radical cations included in this study.

3.1. Assignments. In general, the assignment of the FDMR spectra of the alkane radical cations is based on the following.

(1) Static EPR. Is there agreement with hyperfine coupling constants obtained from CW EPR spectra of alkane radical cations in halogenated matrices? In the case of an unresolved spectrum, does the total width of the FDMR spectrum match that of the CW EPR spectrum?

(2) Elimination. What alternate assignments are possible and can they be ruled out?

(3) Induction. Assignments which are ambiguous, due, for example, to poorly resolved hyperfine structure, are made more certain in the light of positive assignments of other radical cations observed under idential experimental conditions.

Comparison of the FDMR spectrum with EPR spectra of matrix-isolated radical cations is the most direct means of corroborating the assignments of alkane radical cations observed by FDMR. We have carried out original EPR experiments in freon matrices when necessary to supplement information from the literature, especially for $RH^{\bullet+}$ species which are being observed for the first time. The FDMR results are shown as absorption spectra while the static EPR spectra are, for the most part, presented in the familiar first derivative form.

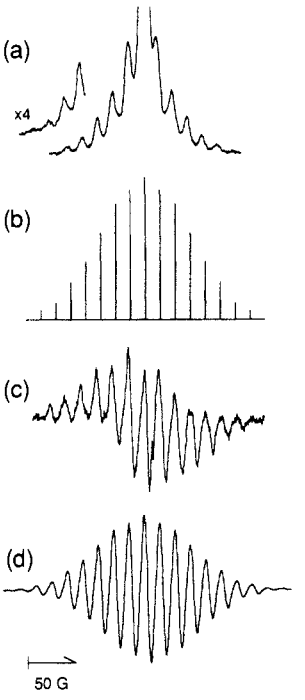

Figure 2. Spectra of the bicyclopentyl radical cation: (a) FDMR spectrum observed at 190 K in *n*-pentane containing 10^{-2} M bicyclopentyl; (*b*) simulated stick spectrum of (a) using the parameters in Table I; (c) static EPR spectrum observed at 150 K in $CFCl_3$; (d) simulated spectrum of (c) using the parameters in Table I.

3.1.1. Liquid-Phase FDMR Spectra of Alkane Radical Cations. 2,2,3,3-Tetramethylbutane$^{\bullet+}$. Figure 1a shows the FDMR spectrum obtained in *n*-pentane containing 10^{-2} M 2,2,3,3-tetramethylbutane. The spectrum consists of an intense central line (off-scale) due to the unresolved EPR lines of the scintillator radical ions superposed on a multiplet of lines (11 observable within the S/N level), coupling constant a = 12.2 G.

Attribution of the multiplet spectrum to the 2,2,3,3-tetramethylbutane radical cation is natural since this signal is not observed in a blank *n*-pentane solution (i.e., *n*-pentane containing only anthracene-d_{10}), and only appears upon addition of 2,2,3,3-tetramethylbutane whose radical cation, presumably, is formed via electron transfer to solvent radical cations. For corroboration of this assignment we can seek to have the observed hyperfine structure duplicated in the CW EPR spectrum of the 2,2,3,3-tetramethylbutane radical cation generated in a freon matrix. One obvious difficultly in making this comparison for liquid-phase FDMR experiments, however, stems from the fact that the CW EPR experiment must be carried out below the melting point of the matrix. The temperature and matrix dependence of the hyperfine interactions can be dramatic, and the present case is a good example.

Figure 1c shows the (first derivative) EPR spectrum of 2,2,3,3-tetramethylbutane$^{\bullet+}$ obtained at 55 K in $CFCl_3$. The seven-line spectrum, a = 27.5 G, matches closely the spectrum (measured at 77 K) reported in the literature and is due to equivalent couplings to six trans C–H protons (one per methyl group) with respect to the central C–C bond.[18,23] This spectrum is indicative of a rigid geometry for the six methyl groups. With increasing temperature the matrix spectrum is seen to undergo a radical transformation, which is fully reversible, to a spectrum with many more lines (13 observable within the S/N level). The spectrum shown in Figure 1d, T = 140 K, is reasonably well simulated (Figure 1e) with the hyperfine parameters used for the stick spectrum in Figure 1b, a = 12.2 G (18 H). Clearly, with increasing temperature the methyl groups begin to rotate freely, resulting ultimately in equivalent couplings to 18 methyl protons.

(17) Toriyama, K.; Nunome, K.; Iwasaki, M. *J. Phys. Chem.* **1981**, *85*, 2149.
(18) Toriyama, K.; Nunome, K.; Iwasaki, M. *J. Chem. Phys.* **1982**, *77*, 5891.
(19) Ohta, N.; Ichikawa, T. *J. Phys. Chem.* **1987**, *91*, 3736.
(20) Shiotani, M.; Yano, A.; Ohta, N.; Ichikawa, M. *Chem. Phys. Lett.* **1988**, *147*, 38.
(21) Nunome, K.; Toriyama, K.; Iwasaki, M. *Tetrahedron* **1986**, *42*, 6315.
(22) Shiotani, M.; Ohta, N.; Ichikawa, T. *Chem. Phys. Lett.* **1988**, *149*, 185.
(23) Nunome, K.; Toriyama, K.; Iwasaki, M. *J. Chem. Phys.* **1983**, *79*, 2499.

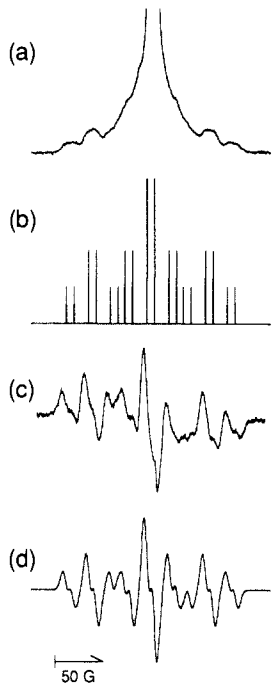

Figure 3. Spectra of the *cis*-bicyclo[4.3.0]nonane radical cation: (a) FDMR spectrum observed at 190 K in *n*-pentane containing 10^{-2} M *cis*-bicyclononane; (b) simulated stick spectrum of (a) using the parameters in Table I; (c) static EPR spectrum observed at 135 K in $CFCl_3$; (d) simulated spectrum of (e) using the parameters in Table I.

Thus, at sufficiently high temperature, the freon matrix EPR spectrum is indeed in agreement with our liquid-phase FDMR spectrum, and our assignment to the 2,2,3,3-tetramethylbutane radical cation is confirmed.

Bicyclophenyl$^{\bullet+}$. Figure 2a shows the FDMR spectrum obtained in *n*-pentane containing 10^{-2} M bicyclopentyl. In addition to the scintillator peak, the spectrum possesses a multiplet of lines (13 observable within the S/N level), evenly spaced, which belongs to the EPR spectrum of the bicyclopentyl radical cation.

The EPR spectrum of bicyclopentyl$^{\bullet+}$ in $CFCl_3$ is temperature dependent and undergoes a reversible change with increasing temperature to a spectrum of fewer lines. The spectrum obtained at 150 K (Figure 2c) can be simulated by two hyperfine couplings, a = 32 G (8 H) and a = 16 G (2 H) (Figure 2d). This is quite consistent with the FDMR spectrum in Figure 2a which is simulated with nearly the same hyperfine parameters, a = 31.2 G (8 H) and a = 15.6 G (2 H) (Figure 2b). This assignment of the couplings is not without ambiguity since, for example, a comparable fit of the experimental spectrum (Figure 2c) can be obtained with the coupling constants, a = 48 G (4 H) and a = 16 G (4 H). An unequivocal assignment of the coupling constants and an understanding of the dynamical effects (temperature dependence) in the EPR spectrum of bicyclopentyl$^{\bullet+}$ require more detailed study. Nevertheless, the obvious agreement between the FDMR and the $CFCl_3$ matrix EPR spectra strongly supports the assignment of the radical cation observed by FDMR to bicyclopentyl$^{\bullet+}$.

In both of these cases, 2,2,3,3-tetramethylbutane$^{\bullet+}$ and bicyclopentyl$^{\bullet+}$, exclusion of alternate radical cation species is trivial. Impurities which might act as hole traps are not a problem when the solute concentration is very low (10^{-2} M) to begin with. Unsaturated species, such as olefin radical cations (due to loss of H_2), are excluded on the basis of the observed hyperfine structure. Furthermore, our previous studies indicate that the solute-derived olefin radical cations are not likely to be formed under these conditions.[10] Other saturated radical cation species (due to rearrangement) can also be ruled out for the reason that they would not be expected to exhibit the observed hyperfine structure.

***cis*-Bicyclo[4.3.0]nonane$^{\bullet+}$.** In many cases, the spectral resolution is inadequate to discern all of the individual lines of the EPR spectrum, as is the case in the FDMR spectrum observed in *n*-pentane containing 10^{-2} M *cis*-bicyclo[4.3.0]nonane (Figure 3a). However, the FDMR spectrum and the $CFCl_3$ matrix EPR spectrum of bicyclononane$^{\bullet+}$ (Figure 3c) still possess enough definition to see that they are well simulated (Figure 3, b and d) by nearly the same hyperfine parameters (see Table I). Again, observation of the matrix EPR spectrum at the highest temperature possible ($CFCl_3$ softens above $\simeq$150 K) leads to good agreement with the liquid-phase FDMR spectrum and allows us to confirm our assignment. The FDMR spectrum of *trans*-bicyclo[4.3.0]nonane$^{\bullet+}$ was also observed under identical conditions. The hyperfine parameters used to simulate its spectrum are given in Table I.

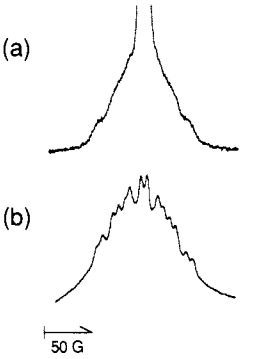

Figure 4. Spectra of the tricyclo[5.2.1.$0^{2,6}$]decane radical cation: (a) FDMR spectrum observed at 190 K in *n*-pentane containing 10^{-2} M tricyclodecane; (b) static EPR spectrum (integrated) observed at 127 K in $CFCl_3$.

Tricyclo[5.2.1.$0^{2,6}$]decane$^{\bullet+}$. Even in cases where the poor resolution of the FDMR spectrum does not allow a meaningful simulation of the hyperfine structure to be made, comparison to the matrix EPR spectrum can be very suggestive. This is illustrated for the case of the FDMR spectrum observed in *n*-pentane containing 10^{-2} M tricyclo[5.2.1.$0^{2,6}$]decane (Figure 4a). Shown in Figure 4b is the (integrated) $CFCl_3$ matrix spectrum of tricyclodecane$^{\bullet+}$. (The matrix EPR spectrum was much more resolved and was reasonably well simulated by the hyperfine parameters found in Table I.) The comparison made in Figure 4 shows clearly that the general shape and width of the matrix EPR spectrum is consistent with that observed by FDMR.

Other Alkane Radical Cations. More examples of FDMR spectra observed in *n*-pentane containing dilute quantities of various alkane solutes are shown in Figures 5 and 6.[24] On the strength of the preceding examples, we can confidently assign the new spectra to the radical cations of the respective solute molecules. The spectra of methylcyclohexane$^{\bullet+}$ and *cis*-1,4-dimethylcyclohexane$^{\bullet+}$ are sufficiently resolved to allow simulation of their hyperfine structure (see Table I), whereas the spectra of *trans*-1,2-dimethylcyclohexane$^{\bullet+}$ and the alicyclic radical cations in Figure 6 are little more than broad shoulders superposed on the scintillator peak. The FDMR spectra of *trans*-1,4-dimethylcyclohexane$^{\bullet+}$ and *cis*-1,2-dimethylcyclohexane$^{\bullet+}$ were not distinguishable from those of their isomeric counterparts. The dissimilarity between the liquid-phase FDMR spectra and matrix EPR spectra for methylcyclohexane$^{\bullet+}$ and 1,2-dimethylcyclohexane$^{\bullet+}$ (see Table I) can again be attributed primarily to freer methyl rotation in the liquid phase. The hyperfine parameters obtained from the liquid-phase FDMR spectrum and matrix EPR spectrum of 1,4-dimethylcyclohexane$^{\bullet+}$, on the other hand, are in reasonably good agreement owing to the lack of any significant coupling to the methyl protons in this case.[22]

3.1.2. Solid-Phase FDMR Spectra of Alkane Radical Cations. Linear Alkane Radical Cations. The distinctive triplet hyperfine structure characteristic of the EPR spectra of *n*-alkane radical cations in low-temperature freon matrices is reproduced in the

(24) The radical cations of methylcyclohexane and adamantane were previously reported to be unobservable under conditions similar to these.[10] Later improvements in the signal-to-noise ratio of our experiment have allowed us to observe them.

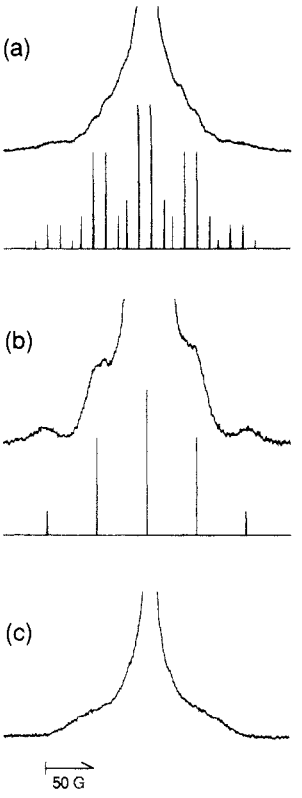

Figure 5. (a) FDMR spectrum observed at 190 K in *n*-hexane containing 10^{-2} M methylcyclohexane; (b) FDMR spectrum observed at 190 K in *n*-pentane containing 10^{-2} M *cis*-1,4-dimethylcyclohexane; (c) FDMR spectrum observed at 190 K in *n*-pentane containing 10^{-2} M *trans*-1,2-dimethylcyclohexane. The hyperfine parameters used for the simulated stick spectra in (a) and (b) are in Table I.

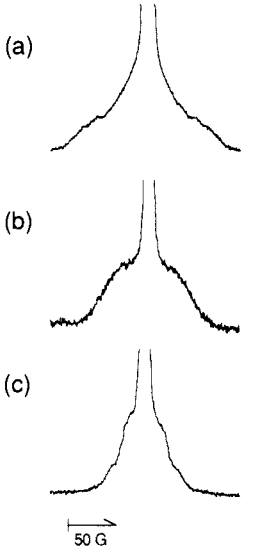

Figure 6. FDMR spectra observed at 190 K in *n*-pentane containing 10^{-2} M (a) perhydrofluorene, (b) adamantane, and (c) bicyclo[3.3.0]octane.

FDMR spectra observed in frozen *n*-alkane solutions (see Table I). The unpaired electron occupies a σ molecular orbital which is delocalized over the entire chain. This gives rise to major hyperfine couplings to the two in-plane end protons, the strength of which decreases with increasing chain length.[17] This trend is illustrated in Figure 7 for *n*-$C_6H_{14}^{\bullet+}$ (a = 41 G) through *n*-$C_9H_{20}^{\bullet+}$ (a = 17 G).

Methyl-Branched Alkane Radical Cations. The FDMR spectra (truncated at the high-field side of the scintillator peak) observed in a variety of frozen methyl-branched alkanes are shown in Figure 8. The static EPR spectroscopy of methyl-branched alkane radical cations in freon matrices is complicated somewhat by strong matrix effects on the hyperfine couplings. Singly methylated alkane

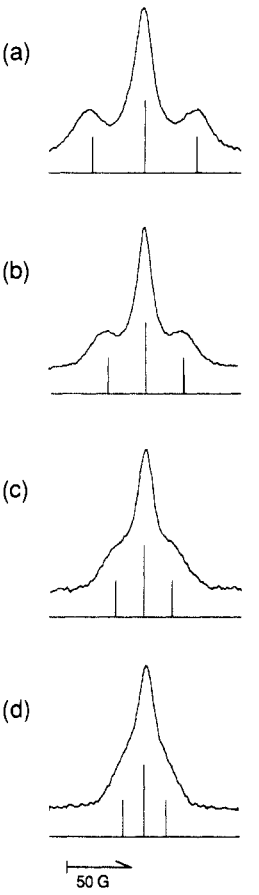

Figure 7. FDMR spectra observed at 35 K in (a) *n*-hexane, (b) *n*-heptane, (c) *n*-octane, and (d) *n*-nonane. The hyperfine parameters used for the simulated stick spectra are in Table I. The FDMR spectra in (a)–(d) have been normalized with respect to the central peak height.

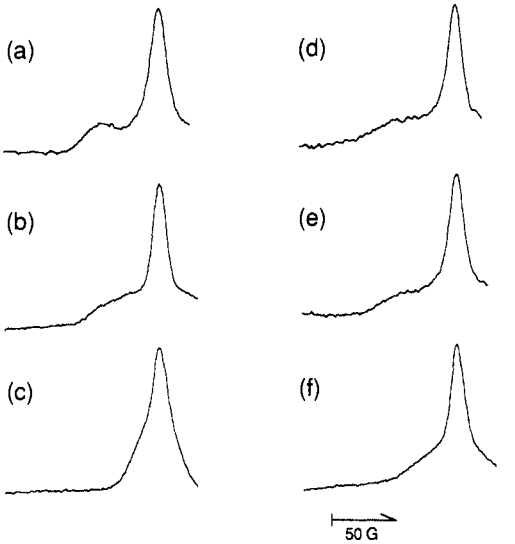

Figure 8. FDMR spectra observed at 35 K in (a) 2-methylhexane, (b) 2-methylheptane, (c) 2-methyldecane, (d) 3-methylpentane, (e) 3-methylhexane, and (f) 3-methyloctane. The spectra in (a)–(f) have been normalized with respect to the central peak height.

cations lower than CH_3–$C_7H_{15}^{\bullet+}$ generally exhibit broad four-line EPR spectra in $CFCl_2CF_2Cl$, indicating that the unpaired electron is more or less confined to one bond joining the tertiary carbon atom and a chain carbon atom, giving rise to relatively large hyperfine couplings (not necessarily equivalent) to three trans C–H_β protons.[19,20,25] The ^1H couplings are extremely sensitive

(25) Toriyama, K.; Nunome, K.; Iwasaki, M. *Chem. Phys. Lett.* **1986**, *132*, 456.

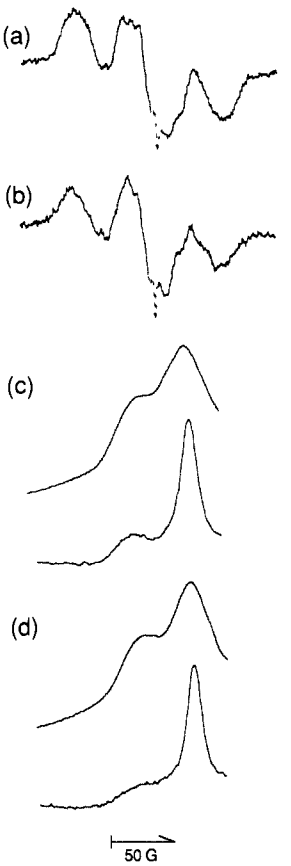

Figure 9. Static EPR spectra of the radical cations of (a) 2-methylhexane and (b) 3-methylhexane observed at 80 K in $CFCl_3$. (c) Top, integrated version of (a); bottom, same as (8a). (d) Top, integrated version of (b); bottom, same as (8e). The broken line in (a) and (b) is due to a color center in the sample cell.

to conformational changes, and thus to the cation's environment. For example, Shiotani and co-workers have reported that upon changing the matrix from $CFCl_2CF_2Cl$ to CF_2BrCF_2Br the EPR spectrum of 3-methylpentane$^{\bullet+}$ changes dramatically from a four-line spectrum to a three-line spectrum.[20] Three-line EPR spectra are also observed for 2-methylhexane$^{\bullet+}$ and 3-methylhexane$^{\bullet+}$ in $CFCl_3$ as illustrated in Figure 9. Comparison of the integrated $CFCl_3$ EPR spectra to the FDMR spectra obtained in 2-methylhexane and 3-methylhexane (Figure 9, c and d) shows the agreement to be quite good. The narrowing of the FDMR spectrum upon going to 3-methyloctane and 2-methyldecane (Figure 8) is consistent with the trend observed for the matrix EPR spectra of several other methyl-branched alkane radical cations higher than CH_3–$C_7H_{18}$$^{\bullet+}$.[19] The total extent of the EPR spectrum decreases with increasing chain length because of the greater delocalization of the singly occupied orbital. We therefore conclude that the EPR signature observed in the FDMR spectra in methyl-branched alkanes again belongs to the solvent radical cation.

Cyclic Alkane Radical Cations. Figure 10 shows the FDMR spectra (truncated at the low-field side of the scintillator peak) observed in three different methylated cyclohexane compounds. The features of the solvent radical cations are not very distinct or well resolved, but with guidance from matrix EPR data the two dimethylcyclohexane radical cation spectra could be simulated reasonably well in fairly good agreement with the matrix hyperfine values (see Table I). *trans*-1,2-Dimethylcyclohexane gave essentially the same result as *cis*-1,2-dimethylcyclohexane, while the solvent radical cation signal in *trans*-1,4-dimethylcyclohexane was too weak to be observed. The FDMR spectrum observed in methylcyclohexane (Figure 10a) is too unresolved to allow simulation of the hyperfine couplings, but the total width of the spectrum is consistent with the EPR parameters measured for the methylcyclohexane radical cation in a halogenated matrix.[22] (The

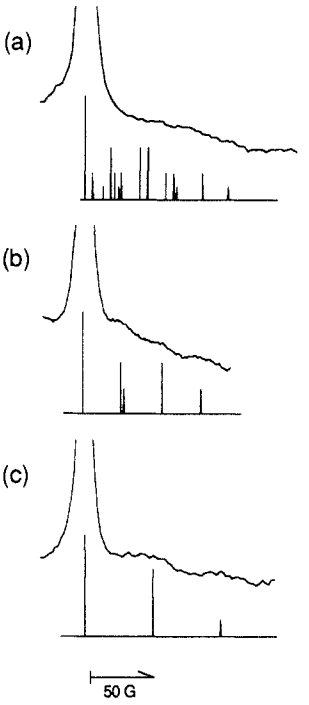

Figure 10. FDMR spectra observed at 35 K in (a) methylcyclohexane, (b) *cis*-1,2-dimethylcyclohexane, and (c) *cis*-1,4-dimethylcyclohexane. The hyperfine parameters used for the simulated stick spectra are in Table I.

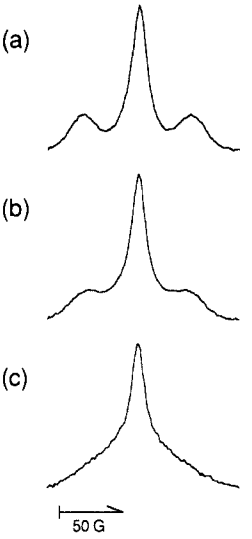

Figure 11. Temperature dependence of the FDMR spectrum observed in *n*-hexane: (a) T = 20 K; (b) T = 88 K; (c) T = 120 K. The spectra in (a)–(c) have been normalized with respect to the central peak height.

parameters used for the simulated stick spectrum in Figure 10a were taken from ref 22.)

3.2. Temperature–Concentration Dependence. Some generalizations are made here about the conditions under which we do observe alkane radical cations by FDMR. However, the ease of observation of RH$^{\bullet+}$ also depends on the alkane under study. Variation of the FDMR results for different alkanes is the subject of section 3.3.

In neat alkane solvents, the solvent radical cation is only observed in frozen samples at low temperatures. The maximum temperature at which a given cation can be observed was determined for only a few cases, but it can vary considerably. In our previous study we found that the *cis*-decalin$^{\bullet+}$ FDMR spectrum can be observed in neat *cis*-decalin at temperatures as high as 150 K, while *trans*-decalin$^{\bullet+}$ is only observed below 100 K.[11] As shown in Figure 11, the *n*-hexane$^{\bullet+}$ FDMR spectrum can be observed above 100 K, but the maximum temperature was difficult to

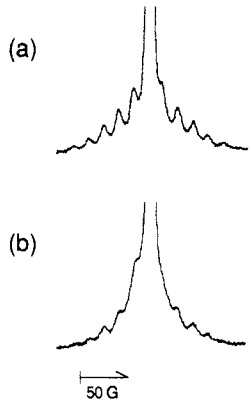

Figure 12. FDMR spectra observed at 195 K in *n*-hexane containing (a) 0.1 M and (b) 0.5 M bicyclopentyl. The spectra in (a) and (b) have been normalized with respect to the central peak height.

determine since the shape of the spectrum also changes with temperature. The $CFCl_3$ matrix EPR spectrum of *n*-hexane$^{\bullet+}$ also becomes less resolved with increasing temperature. The change in coupling constants can be attributed to freer rotation about C–C bonds. A mixture of extended and gauche conformers is also possible. The temperature dependence of the FDMR spectrum in *n*-heptane was similar to that in *n*-hexane.

In only one alkane solvent was the FDMR intensity observed to increase with increasing temperature (in the solid). In cyclopentane at 35 K the center peak of the FDMR spectrum is barely detectable, but it increases in intensity 20-fold at 115 K (and solvent radical cation features are also present). This anomalous temperature dependence was not observed for any other alkane (including half a dozen alkanes which, like cyclopentane, give exceedingly weak scintillator FDMR signals at 35 K). However, as cyclopentane appears to be exceptional in regard to the FDMR results, we choose not to focus on it here.

In the liquid phase, alkane radical cations are observed only under dilute conditions. The effect of increasing concentration on the FDMR spectrum observed in *n*-hexane containing bicyclopentyl is shown in Figure 12. As the solute (bicyclopentyl) concentration increases, the solute cation FDMR intensity decreases. Note that the spectral lines do not appear to broaden. Similar behavior was reported for *cis*-decalin$^{\bullet+}$ and norbornane$^{\bullet+}$.[10] We have not systematically studied the concentration dependence in every case, but loss of FDMR intensity with increasing concentration above 0.1 M seems to be a general rule.

Liquid-phase spectra of alkane radical cations can be observed over a range of temperature, some as high as room temperature. There are sensitivity advantages intrinsic to liquid-phase FDMR at lower temperatures which have little to do with relative cation stability.

3.3. Solute–Solvent Dependence. Various solute/solvent pairs were examined which do not appear in section 3.1.1. In many instances, dilute liquid solutions yield FDMR spectra which do not exhibit any solute cation signal (i.e., only a scintillator peak is observed). The failure to observe the solute cation often may have a trivial explanation. For example, the solute may have a higher ionization potential than the solvent, precluding solute cation formation via electron transfer from solute molecules to solvent radical cations. Alternatively, the solute cation may simply have a very diffuse EPR spectrum (many lines of low intensity) and is therefore hard to see. One need only compare, e.g., the spectra of methylcyclohexane$^{\bullet+}$ (Figure 5a) and bicyclopentyl$^{\bullet+}$ (Figure 2a) to appreciate how the number of lines and degree of resolution in the EPR spectrum affect the FDMR sensitivity. Unfortunately, sufficient information about the relative ionization potentials and the EPR spectra are often lacking.

In some cases where a solute alkane fails to give a cation signal in the FDMR spectrum, "trivial" explanations seem not to apply. A prime example is *trans*-decalin. The gas-phase ionization potential of *trans*-decalin is nearly the same as that of *cis*-decalin (9.35 eV) and considerably lower than that of many possible solvents (e.g., *n*-pentane: IP = 10.2 eV). The EPR spectrum of *trans*-decalin$^{\bullet+}$ observed in low-temperature solids is virtually identical with that of *cis*-decalin$^{\bullet+}$.[11,12] Yet, in contrast with *cis*-decalin$^{\bullet+}$, the FDMR spectrum of *trans*-decalin$^{\bullet+}$ is not observed at all in the liquid phase and can only be observed at the lowest temperatures (<100 K) in the solid phase where it is still an order of magnitude less intense than *cis*-decalin$^{\bullet+}$.

Table II. Effect of Alkane Solutes on I_{FDMR}, I_{fl}, and I_{FDMR}/I_{fl} in *n*-Pentane Solvent (T = 190 K, [solute] = 10^{-2} M)

solute	I_{FDMR}	I_{fl}	I_{FDMR}/I_{fl}[a]
none	287	1540	0.19
cis-decalin	397	1880	0.21
trans-decalin	62	1190	0.052
cyclohexane	47	880	0.053
bicyclo[2.2.2]octane	52	1040	0.050
bicyclo[3.3.0]octane	262	1560	0.17
2,2,3,3-tetramethylbutane	276	1460	0.19
bicyclopentyl	270	1420	0.19
3-methyloctane	238	1260	0.19
bicyclohexyl	233	1250	0.19
cycloheptane	233	1420	0.16

[a] This quantity was more reproducible from run to run than either I_{FDMR} or I_{fl}. Uncertainty is ±0.01.

In further contrast with *cis*-decalin, small amounts (10^{-2} M) of *trans*-decalin cause a pronounced decrease in the intensity of the central FDMR peak (I_{FDMR}) due to the anthracene ions in the liquid phase.[26] The total fluorescence intensity (I_{fl}, measured off-resonance and integrated over the time window of the boxcar detector: 100–200 ns) decreases as well, as does the ratio I_{FDMR}/I_{fl}. Other alkanes found to produce this effect include cyclohexane, bicyclo[2.2.2]octane and, to a lesser extent, *trans*-1,4-dimethylcyclohexane. The cyclohexane and bicyclo[2.2.2]octane radical cations are not observed in liquid-phase FDMR experiments. *trans*-1,4-Dimethylcyclohexane$^{\bullet+}$ could be observed but was less intense than *cis*-1,4-dimethylcyclohexane$^{\bullet+}$. The quantities I_{FDMR}, I_{fl}, and I_{FDMR}/I_{fl} are examined for a variety of solutes in *n*-pentane in Table II.

The FDMR intensity observed in solid-phase experiments also varies dramatically for different alkanes. In neat alkanes (T = 35 K, anthracene-d_{10} concentration = 10^{-3} M), I_{FDMR} (height of the center peak), was found to vary over at least two orders of magnitude, depending on the solvent. I_{fl} increased or decreased roughly in correspondence with I_{FDMR}. Variations are found in homologous series. I_{FDMR} was nearly an order of magnitude greater in cycloheptane than in cyclopentane or cyclohexane. In the series *n*-C_xH_{x+2}, x = 5–13, the ratio between the high, I_{FDMR} (x = 7), and the low, I_{FDMR} (x = 12), was approximately 18. Variations occur between pairs of isomers. The ratio I_{FDMR}(cis)/I_{FDMR}(trans) was approximately 10 for decalins and for the isomers of 1,4-dimethylcyclohexane. The three compounds with the lowest values of I_{FDMR}/I_{fl} in Table II are among the solvents which give the weakest FDMR signals in solid-phase experiments.

I_{FDMR} is not always stronger is glassy alkanes than in polycrystalline ones, nor vice versa. Simple structural changes do not consistently produce the same effect. For example, I_{FDMR} is approximately 25 times greater in methylcyclohexane than in cyclohexane, but it is equally weak (at 35 K) in methylcyclopentane and cyclopentane. It was found that an admixture of a few percent of *cis*-decalin in those solvents found to give a weak FDMR response when neat (e.g., isopentane, isooctane, methylcyclopentane) gave rise to a fairly strong spectrum possessing the features of the *cis*-decalin radical cation.

3.4. Ion–Molecule Reactions of Radical Cations in the Condensed Phase. In the previous sections we have illustrated the conditions under which alkane radical cations can be observed by FDMR. These findings are themselves clues about the nature and fate of alkane radical cations in irradiated alkanes. The most important findings are that isolation of RH$^{\bullet+}$ from the parent RH and/or low temperatures are needed to stabilize alkane radical

(26) This effect of *trans*-decalin has also been noted by Melekhov et al.[13]

cations. Thus, we are forced to consider some bimolecular decay channel which competes with geminate ion recombination and shortens the radical cation lifetime. Also, there is a considerable diversity among different alkanes that must be accounted for. In this section we show that these facts, in conjunction with previous experimental observations, are consistent with the conclusion that alkane radical cations undergo ion–molecule reactions with neutral alkane molecules.

Rapid decay of $RH^{\bullet+}$ via reactions other than recombination with its geminate partner is indicated, for example, by the concentration dependence of solute cation FDMR signals in the liquid phase, illustrated in this study for bicyclopentyl in *n*-hexane. The loss of signal due to bicyclopentyl$^{\bullet+}$ with increasing solute concentration requires a decay channel involving a bimolecular reaction between bicyclopentyl$^{\bullet+}$ and neutral solute (bicyclopentyl) molecules.

Resonant Charge Transfer. The possible bimolecular reactions are ion–molecule reactions (vide infra) and fast charge transfer. Fast resonant charge transfer (eq 9) has been advanced to explain

$$RH^{\bullet+} + RH \rightarrow RH + RH^{\bullet+} \quad (9)$$

some curious observations indicating fast positive charge transport in several hydrocarbons, with cyclohexane and *trans*-decalin being the most notable examples.[27] Fast resonant charge transfer would tend to delocalize the electron spin and, in the limit of fast electron hopping, narrow the EPR spectrum into a single, narrow line.

This fast resonant charge transfer can be ruled out by several experimental observations and by our FDMR results. Most significant is the observation that one cannot observe, e.g., *trans*-decalin$^{\bullet+}$ in a solution of *n*-pentane where the decalin solute is the species (trap) with the lowest ionization potential. If only resonant charge transfer prevented us from observing radical cations, then we should be able to observe the radical cation of any alkane diluted in a solvent whch has a higher ionization potential. This is clearly not the case. Furthermore, there is no evidence for the onset of spectral narrowing (e.g., loss of resolution or broadening of individual lines) in Figure 12 as the bicyclopentyl concentration is increased. The bicylopentyl$^{\bullet+}$ signal just decreases in intensity. The same behavior was observed for *cis*-decalin$^{\bullet+}$ and norbornane$^{\bullet+}$.[10] The persistence of resolved hyperfine structure is indication that the radical cation remains localized. In addition, it seems improbable that resonant charge transfer would become slower with decreasing temperature, which one would have to postulate to explain the observation of resolved $RH^{\bullet+}$FDMR spectra in neat alkane solids at low temperatures.[28]

One would expect the effects of electron delocalization to be manifested in other experiments as well. In particular, the degree of delocalization of the unpaired electron will have a dramatic effect on the electronic absorption spectra of radical cations. Parallel studies of alkane radical cations in freon matrices by EPR and optical absorption spectroscopy demonstrate that the absorption maxima shift to longer wavelength with increasing electron delocalization. For example, λ_{max} of straight chain and singly methylated alkane radical cations increases with increasing chain length, extending through the visible region and near-infrared, while the λ_{max} of highly branched radical cations such as dimethylbutane$^{\bullet+}$, trimethylbutane$^{\bullet+}$, and tetramethylbutane$^{\bullet+}$ is approximately 260 nm.[29] These trends are in strict accord with the trends in spin densities deduced from the EPR data. Therefore, fast resonant charge transfer in concentrated alkane solutions, resulting in charge delocalization over several molecules, could red-shift the alkane radical cation absorption spectrum hundreds of nanometers. The exact magnitude of such an effect would depend on the actual rate of electron hopping or the strength of the electronic interaction (i.e., between cations and the solvent molecules). However, the few reported cases in which alkane radical cations have been observed in irradiated alkanes by optical absorption do not reveal such dramatic red shifts.

Finally, fast resonant charge transfer cannot account for the most significant finding of transient absorption studies of irradiated alkanes, which is that $RH^{\bullet+}$ decays faster than the solvated electrons.[3-7,9] We are left with ion–molecule reactions as the only viable bimolecular mechanism of $RH^{\bullet+}$ decay that can compete with cation–electron recombination.

Ion–Molecule Reactions. What do we know about ion–molecule reactions in the condensed phase? Ion–molecule mechanisms involving transfer of $H^{\bullet}$, H^+, H^-, H_2, and H_2^- have all been invoked to explain various experimental observations in condensed-phase hydrocarbons.[21,30-35] This list also includes, for example, ion–molecule reactions between saturated and unsaturated species. H_2 transfer obviously requires an appropriate H_2 acceptor such as an olefin, olefin cation, or cyclic alkane, as in reactions of cyclopropane with alkane radical cations.[32]

$$n\text{-}C_6H_{14}^{\bullet+} + c\text{-}C_3H_6 \rightarrow C_6H_{12}^{\bullet+} + n\text{-}C_3H_8 \quad (10)$$

The only ion–molecule reactions between alkane radical cations and alkane molecules which are equally general for acyclic alkanes and for which significant experimental evidence exists are those which convert alkane radical cations into alkyl radicals, i.e., proton transfer (eq 11) and the symmetric process yielding the same

$$RH^{\bullet+} + RH \rightarrow R^{\bullet} + RH_2^+ \quad (11)$$

products via hydrogen atom transfer to the radical cation (eq 12).

$$RH^{\bullet+} + RH \rightarrow RH_2^+ + R^{\bullet} \quad (12)$$

The molecular ions, RH_2^+, are not observed in mass spectral studies of pure alkanes in the gas phase with the exception of CH_5^+ in the case of methane.[36] Estimates, based on gas-phase proton affinities, have been made in select cases for the heat of reaction for (11). For cyclohexane, proton transfer is estimated to be endothermic by 15 kcal/mol,[37] while for *n*-butane it has been estimated to be approximately thermoneutral.[36] Unfortunately, the needed thermochemical data (e.g., proton affinities) are not available for most alkanes.

Perhaps the most relevant work illustrating the importance of ion–molecule reactions of alkane radical cations in the condensed phase are the low-temperature studies of Iwasaki and Toriyama who have investigated the static EPR signals induced by ionizing radiation in solutions of alkanes in halogenated matrices and zeolites and in neat *n*-alkane crystals.[2,18,21,30,38,39] These studies establish that (1) most of the alkyl radicals are formed from radical cations since the radical produced reflects the spin density of the radical cation, and (2) radical cations are converted into radicals via biomolecular reactions with alkane molecules.

Other relevant observations illustrate that alkyl radicals are produced by a fast process since radicals can be observed on the picosecond time scale.[9] In another study using time-resolved EPR, we have shown that the cyclohexyl radical yield is not affected by cation or electron scavengers.[40] This is consistent with the

(27) Warman, J. M. *The Study of Fast Processes and Transient Species by Electron Pulse Radiolysis*; Baxendale, J. H., Busi, F.; Eds.; Reidel: Boston, 1981; p 433.

(28) If resonant charge transfer is feasible in liquids, then, as suggested by Warman,[27] one might expect it to be even more facile in low-temperature hydrocarbon solids based on the argument that slower geometric relaxation of the cation following ionization could enhance the Franck–Condon factor for electron transfer for a considerable length of time.

(29) Ichikawa, T.; Ohta, N. *J. Phys. Chem.* **1987**, *91*, 3244.

(30) Toriyama, K.; Nunome, K.; Iwasaki, M. *J. Am. Chem. Soc.* **1987**, *109*, 4496.

(31) Ausloos, P.; Scala, A. A.; Lias, S. G. *J. Am. Chem. Soc.* **1967**, *89*, 3677.

(32) Rzad, S. J.; Schuler, R. H. *J. Phys. Chem.* **1968**, *72*, 228.

(33) Collin, G. J.; Ausloos, P. *J. Am. Chem. Soc.* **1971**, *93*, 1336.

(34) Shida, T.; Egawa, Y.; Kubodera, H. *J. Chem. Phys.* **1980**, *73*, 5963.

(35) Fujisawa, J.; Sato, S.; Shimokoshi, K.; Shida, T. *J. Phys. Chem.* **1985**, *89*, 5481.

(36) Ausloos, P. *Radiat. Phys. Chem.* **1982**, *20*, 87.

(37) Ausloos, P.; Rebbert, R. E.; Schwarz, F. P.; Lias, S. G. *Radiat. Phys. Chem.* **1983**, *21*, 27.

(38) Iwasaki, M.; Toriyama, K.; Nunome, K. *Faraday Discuss. Chem. Soc.* **1984**, *78*, 1.

(39) Toriyama, K.; Nunome, K.; Iwasaki, M. *J. Phys. Chem.* **1986**, *90*, 6836.

idea that conversion of radical cations into radicals is fast.

Diversity in $RH^{\bullet+}$ Reactivity. The propensity of $RH^{\bullet+}$ species to undergo ion–molecule reactions must vary greatly in light of the wide variation in the observability of alkane radical cations by FDMR and by optical absorption methods. The liquid-phase FDMR results indicate that in most cases solute radical cations undergo ion–molecule reactions with neutral solute molecules but not with solvent molecules. However, exceptions to this rule may explain why some solute radical cations are not observed; e.g., *trans*-decalin$^{\bullet+}$ may react with any neutral alkane molecule. The most suspect cases, as mentioned above, are those where the addition of the solute does not give rise to a solute cation signal and results in a decrease in the intensity of the central FDMR peak due to the scintillator radical cation and radical anion (see Table II). Destruction of radical cations due, for example, to competition of reactions 13 and 14 (RH = alkane solvent, SH

$$RH^{\bullet+} + SH \rightarrow RH + SH^{\bullet+} \quad (13)$$

$$SH^{\bullet+} + RH \rightarrow S^{\bullet} + RH^{2+} \quad (14)$$

= alkane solute) in the scheme outlined in eq 1–8 would decrease the yield of recombination reactions involving $A^{\bullet+}$ or $A^{\bullet-}$.

The decay of $RH^{\bullet+}$ is slowed down in most solvents with decreasing temperature, as evidenced by our ability to detect many alkane radical cations in neat alkanes in low-temperature solids. However, even at 35 K and colder, the observed FDMR signal intensity is extremely variable depending on the alkane solvent. The variation in solid-phase FDMR intensity is due primarily, if not solely, to variation in the yield of the excited scintillator A* from reaction 7. This is supported by the observation that, in all cases, an intense central FDMR peak is accompanied by solvent radical cation features. In frozen alkanes where the solvent radical cation signals are exceedingly weak or undetectable, the central peak intensity is correspondingly low. This is in contrast with liquid-phase FDMR where a relatively intense central peak is obtained whether or not wing features due to $RH^{\bullet+}$ species are observed. This difference must be due to changes in the relative contributions of the various reactions giving rise to FDMR (e.g., less contribution from reaction 6 in solids compared to liquids) as a result of temperature and viscosity effects on diffusion and charge mobility. The increase in FDMR intensity observed upon addition of a few percent *cis*-decalin to, e.g., isopentane (at 35 K), is likewise attributable to a recombination reaction between an alkane radical cation (*cis*-decalin$^{\bullet+}$) and $A^{\bullet-}$ as shown by the presence of the *cis*-decalin$^{\bullet+}$ features in the spectrum. Contributions to the FDMR signal from reactions 5 and 6 are apparently small or negligible; therefore variations in the yields from reactions 5 and 6 cannot help to account for the solvent dependence of the solid-phase FDMR results.

A large number (>30) of alkanes have been investigated in an attempt to understand the cause of the solvent dependence of the $RH^{\bullet+} + A^{\bullet-}$ FDMR intensity in neat solids. One possible explanation is that, as in the liquid phase, different alkane radical cations show different propensities for undergoing ion–molecule reactions with alkane molecules; i.e., even at very low temperatures some radical cations still react too fast to be observed during the FDMR observation time window (20–100 ns). We have already noted the contrasting $RH^{\bullet+}$ reactivity in the liquid phase for even closely related species such as cis/trans isomers, and solid-phase results parallel those in liquids. For example, observation of the radical cation of the cis isomer of 1,4-dimethylcyclohexane is more facile than that of the trans isomer in the liquid phase and in the neat solid at low temperature. Similar results for *cis*- and *trans*-decalin were discussed at length in our previous report.[11] Cyclohexane is one more example. Alkane radical cations which give weak (or negligible) FDMR signals in dilute liquid solutions also give weak signals in frozen solids.

An alternative explanation is that the solvent dependence of the FDMR intensity reflects changes in the rate or yield of geminate recombination due to factors such as variation of the average separation distance between $RH^{\bullet+}$ and $A^{\bullet-}$ with the electron mobility in different solvents or different Franck–Condon factors (matching of states) for reverse electron transfer ($A^{\bullet-}$ to $RH^{\bullet+}$). The latter has been suggested to influence the yield of trapped electrons in organic glasses and could be important, especially if single-step electron tunneling is a major mode of electron return to the radical cation.[41] Unfortunately, the exact nature of charge recombination in solids is not well known, i.e., whether electron tunneling dominates or whether some positive charge mobility persists in the absence of diffusion. This issue requires further study.

There is not a clear correlation between our solid-phase FDMR results and electron mobilities in alkanes (extrapolating from known mobilities in liquids). For example, isooctane is one of the highest mobility solvents of the alkanes included in our study, and *trans*-decalin is one of the lowest.[27] Yet both of these solvents give very weak FDMR signals (i.e., at 35 K). While greater excursions in the magnitude of the electron mobility (the limiting case being methane) could have a dramatic effect on the FDMR intensity, the small spread in mobilities encountered in our study is probably insignificant. The negative effect of a small Franck–Condon factor on the driving force for reverse electron transfer (and thus the rate) should tend to be offset by increasing ΔIP, the difference between the ionization potentials of the scintillator and the alkane host. Admittedly, such factors that could affect the yield of geminate recombination are difficult to evaluate, but they do not seem sufficient to explain the variation of the FDMR intensity in different alkanes.

The evidence that radical cations which are not observed in liquid-phase experiments have a vanishingly small FDMR response in low-temperature solids (and vice versa) suggests that a common mechanism, i.e., ion–molecule reactions, is responsible for the diversity in both phases. It is not clear what factors might govern the reaction rates of different radical cations. While it would be interesting to examine the proton affinities for all of the alkanes in this study (if they were available), this consideration seems unlikely to tell the whole story. For example, the gas-phase proton affinities for cyclohexane and *n*-butane lead one to predict that proton transfer should be more facile for *n*-butane than for cyclohexane (vide supra). Yet, cyclohexane$^{\bullet+}$ is one of the least stable alkane radical cations judging from the FDMR results, less stable than straight-chain cations such as *n*-pentane$^{\bullet+}$ and *n*-hexane$^{\bullet+}$. Equally remarkable is the marked contrast between the observability of radical cations such as *cis*- and *trans*-decalin$^{\bullet+}$, whose proton affinities would not be expected to be very different.

The regiospecificity of alkyl radical formation in *n*-alkanes led Iwasaki and Toriyama to propose a mechanism of proton loss occurring in radical cations of linear alkanes from the site of maximum spin density.[2,39] On the other hand, reactions of certain radical cations (e.g., cyclopentene oxide$^{\bullet+}$) to form radicals different from the one expected on the basis of maximum spin density appear more consistent with a mechanism involving H-atom transfer to the radical cation.[42] The regiospecificity for H abstraction reactions could be due to steric and geometrical considerations. The observability of alkane radical cations by FDMR does not strictly correlate with the degree of localization or delocalization of the spin density in the radical cation, nor does it exhibit any simple relationship to molecular structure. The (kinetic and thermodynamic) factors governing the propensity of radical cations to undego ion–molecule reactions is an intriguing issue which must await further study. Theoretical investigations could provide needed guidance.

Ion–molecule reactions are widespread in more polar systems. Ion–molecule reactions of a variety of heteroatom-containing radical cations have been studied, e.g., radical cations of ethers, thioethers, and amines.[42–47] Proton transfer to electronegative

(40) Werst, D. W.; Trifunac, A. D. *Chem. Phys. Lett.* **1987**, *137*, 475.

(41) Willard, J. E. *Radiation Chemistry: Principles and Applications*; Farhataziz, Rodgers, M. A. J., Eds.; VCH Publishers: New York, 1987; p 395.

(42) Williams, F.; Qin, X.-Z. *Radiat. Phys. Chem.* **1988**, *32*, 299.

(43) Qin, X.-Z.; Meng, Q.-c.; Williams, F. *J. Am. Chem. Soc.* **1987**, *109*, 6778.

atoms such as oxygen or nitrogen is generally thought to be faster than proton transfer to carbon centers, owing to the availability of a localized electron pair in the former case.[47] Our study raises the possibility that proton transfer to carbon centers may also be quite fast in some cases. An important question for our future study is whether stabilization of radical cations at low temperature is also possible in neat alcohols, ethers, etc., allowing their study by FDMR.

The importance of ion–molecule reactions in the overall chemistry induced by ionizing radiation in hydrocarbons remains to be seen. The fact that the detection sensitivity of the FDMR technique depends on the lifetime of the radical ion species introduces a bias toward longer lived ion pairs. In the FDMR experiment electron scavenging by the scintillator gives rise to less mobile scintillator anions, extending the time available for the partner alkane radical cations to react. This is at once an advantage and a disadvantage of the technique. Delaying recombination amplifies the differences in reactivity of radical cations of different alkanes. But the fact that FDMR only probes a small fraction of events occurring relatively late in time makes it difficult to obtain quantitative estimates of the relative yields of various reaction pathways.

4. Conclusions

In this paper we have discussed various optically detected EPR observations of alkane radical cations in liquid and solid hydrocarbons. We conclude that *ion–molecule reactions* such as proton transfer or H-atom transfer account for the transient nature of alkane radical cations in hydrocarbons. The details of the ion–molecule reactions of alkane radical cations are yet to be fully delineated since factors in addition to molecular shape and spin density in the radical cation must be considered.

Acknowledgment. J. Gregar provided us with the Suprasil FDMR and EPR sample cells. We thank R. H. Lowers for his skillful operation of the Van de Graaff and other technical support and acknowledge him upon his retirement for his many years of valued service and friendship. We acknowledge helpful discussions with X.-Z. Qin, M. C. Sauer, Jr., and C. D. Jonah.

Registry No. 2,2,3,3-Tetramethylbutane radical cation, 68842-40-0; bicyclopentyl radical cation, 75840-32-3; *cis*-bicyclo[4.3.0]nonane radical cation, 123807-66-9; tricyclo[5.2.1.$0^{2,6}$]decane radical cation, 123807-67-0; methylcyclohexane radical cation, 82166-21-0; *cis*-1,4-dimethylcyclohexane radical cation, 123807-68-1; *trans*-1,2-dimethylcyclohexane radical cation, 121054-99-7; perhydrofluorene radical cation, 123807-69-2; adamantane radical cation, 123726-15-8; bicyclo[3.3.0]octane radical cation, 123807-70-5.

(44) Shiotani, M.; Nagata, Y.; Tasaki, M.; Sohma, J.; Shida, T. *J. Phys. Chem.* **1983**, *87*, 1170.
(45) Kubodera, H.; Shida, T.; Shimokoshi, K. *J. Phys. Chem.* **1981**, *85*, 2583.
(46) Lewis, F. *Acc. Chem. Res.* **1986**, *19*, 401.
(47) Kresge, A. J. *Acc. Chem. Res.* **1975**, *8*, 354.

Adsorption and Reactions of Cyclic Sulfides on Mo(110)

Maria José Calhorda,[†,‡] Roald Hoffmann,*[,‡] and Cynthia M. Friend[§]

Contribution from the Department of Chemistry and Materials Science Center, Cornell University, Ithaca, New York 14853-1301, and Department of Chemistry, Harvard University, Cambridge, Massachusetts 02138. *Received December 12, 1988*

Abstract: Molecular orbital calculations of the chemisorption and reactivity of ethylene sulfide and trimethylene sulfide on Mo(110) are presented and compared to similar binding in model-discrete Mo complexes. Our calculations suggest preferred bonding of the cyclic sulfides on 2- or 3-fold sites of the surface, by the expected S-lone pair donor mechanism. The concerted elimination of ethylene or cyclopropane is much easier on the surface than it is in model organometallic molecules. The activation barrier for ethylene sulfide decomposition calculated is substantially smaller than that for trimethylene sulfide. Various nonconcerted mechanisms and the role of coadsorbed sulfur and hydrogen are also probed.

Hydrodesulfurization is a widely used process by which fuel feedstocks react with a molybdenum sulfide catalyst to afford hydrocarbons with lower sulfur content. Several kinds of sulfur derivatives, both aromatic and aliphatic, are found in the raw materials, and considerable effort has been dedicated toward understanding how the reactions occur.[1] Often, simpler models than the actual catalyst are used for that, namely single-crystal transition-metal surfaces.[2]

The molybdenum(110) face has been chosen, due to its stability toward reconstruction, by Friend and co-workers to study systematically the reactions of cyclic sulfides[3] and linear thiols.[4] With the help of several complementary experimental techniques such as temperature-programmed desorption, X-ray photoelectron, and high-resolution electron energy loss spectroscopy, they have been able to establish three distinct reactivity patterns. These three pathways are indicated in **1**, depicting how trimethylene sulfide reacts after adsorption onto the Mo(110) face.

Pathway A leads to cyclopropane formation by intramolecular elimination. An intermediate adsorbed thiolate species is formed in B. The same intermediate is detected directly when a different precursor, propanethiol, reacts with the surface.

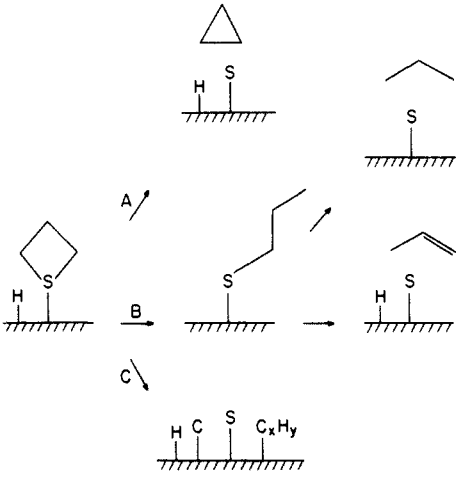

1

[†] Permanent address: Centro de Quimica Estrutural, Instituto Superior Técnico, 1096 Lisbon Codex, Portugal.
[‡] Cornell University.
[§] Harvard University.

0002-7863/90/1512-50$02.50/0